Proc. Natl. Acad. Sci. USA
Vol. 90, pp. 352–356, January 1993
Medical Sciences

Plasmacytoid differentiation of Epstein–Barr virus-transformed B cells *in vivo* is associated with reduced expression of viral latent genes

(lymphoproliferative disorders/severe combined immunodeficiency mice/lymphoblastoid cell lines)

ROSEMARY ROCHFORD, MONTE V. HOBBS, JEANNE-LUCE GARNIER*, NEIL R. COOPER, AND MARTIN J. CANNON†

Department of Immunology, The Scripps Research Institute, La Jolla, CA 92037

Communicated by Frank J. Dixon, October 5, 1992

ABSTRACT **The Epstein–Barr virus (EBV)-associated B-cell lymphoproliferative disorders that arise in immunosuppressed individuals are considered to resemble EBV-transformed *in vitro* lymphoblastoid cell lines (LCLs) with a mature activated B-cell phenotype. In this study of human lymphoproliferative disorders in the severe combined immunodeficiency mouse model, however, we demonstrate that EBV-infected tumor cells are not LCL-like but are predominantly plasmacytoid and that this phenotype correlates with reduced expression of EBV latent genes. B-cell tumors developed within 3–6 weeks after injection of LCLs into severe combined immunodeficiency mice. The tumors and the injected LCLs were analyzed by flow cytofluorometry for B-cell differentiation and activation markers and by ribonuclease protection assay for cellular and viral gene expression. No differences in the expression of CD19 and CD21 were observed. However, a decrease in CD23, CD11a (lymphocyte function-associated antigen LFA-1), and CD58 (LFA-3) expression and an increase in CD38 (a plasma-cell-associated antigen), CD54 (intracellular adhesion molecule ICAM-1), and HLA class I in the tumor cells relative to the LCLs was observed. Two-color flow cytofluorometric analysis showed that the predominant population (>80%) in LCLs was $CD23^{hi}/CD38^{lo}$ and that the major population in LCL-derived tumors was $CD23^{lo}/CD38^{hi}$. Cell cycle analysis showed that, in contrast to actively cycling LCLs, the majority of tumor cells had exited the cell cycle and were restricted to G_0/G_1 phase. Finally, and most important, a reduction in mRNA for the EBV latent genes EBV nuclear antigen 2 (EBNA2) and latent membrane protein (LMP1) was observed in the tumors.**

In humans with latent/persistent Epstein–Barr virus (EBV) infection, outgrowth of infected B cells is thought to be controlled by virus-specific cytotoxic T-cell surveillance; indeed, abrogation of T-cell immunity frequently results in the appearance of the oligoclonal or monoclonal EBV-associated B-cell lymphoproliferative disorders (LPDs) that constitute a major complication in immunocompromised organ allograft recipients (for review, see refs. 1 and 2). The association of EBV with LPDs is based on serologic evidence of EBV infection and the detection of viral DNA and the EBV-encoded antigens EBV nuclear antigen (EBNA) 1, EBNA2, and latent membrane protein (LMP) in the tumors (2, 3).

Human LPD lesions are considered to be the *in vivo* equivalent of *in vitro* lymphoblastoid cell lines (LCLs), which express 10 EBV latent genes: EBNA1, -2, -3A, -3B, and -3C; LMP1 and -2; leader protein; and two untranslated RNA species (EBERs; for review, see ref. 4). EBNA1 is the only viral gene product required for maintenance of the episomal EBV genome (5, 6). EBNA2 and LMP1 are effectors of growth transformation (7–9). The functions of the other genes have not been clearly elucidated. Immortalization of B cells is accompanied by phenotypic changes, including high expression of the B-cell activation antigen CD23 and adhesion molecules CD11a (lymphocyte function-associated antigen LFA-1), CD54 (intracellular adhesion molecule ICAM-1), and CD58 (LFA-3) (10, 11).

Although phenotypic analysis of LPDs has suggested similarities with LCLs, based on positive immunohistology for CD23, CD58 (LFA-3), and CD54 (ICAM-1) in three lesions (12), other studies found positive CD23 expression in only five of nine LPD lesions (13), and three lesions were positive for the expression of CD38, a surface antigen associated with plasma-cell formation (13). Furthermore, histopathologic analysis characterizes LPD as polymorphic B-cell immunoblasts with variable degrees of plasmacytoid features (14–16).

In this study, we have addressed the question of whether EBV-associated LPDs are mature LCL-like activated B cells or represent a more differentiated plasmacytoid phenotype, by examining patterns of cellular and viral gene expression in EBV-induced LPDs of severe combined immunodeficiency/human (SCID/hu) chimeric mice, a model that has been shown to be remarkably similar to human posttransplant LPDs (17–19). Recent studies on EBV-induced tumor formation in SCID/hu chimeric mice have shown that CD23 and CD20 expression by the tumor cells is greatly reduced relative to donor-matched LCLs (20, 21) and that tumor cells have a plasmacytoid morphology (17, 18). We injected LCLs into SCID mice and compared the resultant tumor cells to the input LCL. Analysis of LCL-derived tumors, rather than tumors arising in SCID mice engrafted with human peripheral blood (17, 18, 20), ensures that all tumor cells are EBV-infected and avoids the possible presence of reactive (i.e., uninfected) B-cell populations. We present data to show that phenotypic changes in the tumor cells consistent with a terminally differentiated plasma cell were observed and that the tumor cells have significantly reduced EBNA2 and LMP1 gene expression relative to the input LCLs, indicating that

The publication costs of this article were defrayed in part by page charge payment. This article must therefore be hereby marked "*advertisement*" in accordance with 18 U.S.C. §1734 solely to indicate this fact.

Abbreviations: EBV, Epstein–Barr virus; LPD, lymphoproliferative disorder; LCL, lymphoblastoid cell line; SCID, severe combined immunodeficiency; hu, human; EBNA, EBV nuclear antigen; LFA, lymphocyte function-associated antigen; ICAM, intracellular adhesion molecule; FCF, flow cytofluorometry; IF, immunofluorescence; mAb, monoclonal antibody; rp, ribosomal protein; LMP, latent membrane protein.

*Present address: Unite de Recherches en Nêphro-Urologie, Transplantation et Immunologie Clinique, Pavillon P, Hôpital Edouard Herriot, Place d'Arsonval, 69437, Lyon Cedex 03, France.

†To whom reprint requests should be addressed at: Department of Immunology (IMM19), The Scripps Research Institute, 10666 North Torrey Pines Road, La Jolla, CA 92037.

reduction in EBV latent gene expression correlates with B-cell differentiation.

MATERIALS AND METHODS

Lymphoblastoid Cell Lines. EBV-transformed LCLs were prepared by infection of peripheral blood lymphocytes with B95-8 virus in the presence of cyclosporin A (Sandoz Pharmaceutical) as described (22). Five donors were used to establish five lines: JR, KR, LG, TL, and EW. These lines were passaged for 3–6 months in culture before injection into C.B-17 *scid/scid* mice (SCID) (23). Cell lines were maintained in RPMI 1640 medium/10% (vol/vol) fetal calf serum, supplemented with antibiotics and glutamine.

Mice. SCID mice were bred in the Scripps Research Institute breeding colony. Eight-week-old mice were injected intraperitoneally with 3×10^6 cells for each LCL. Mice were sacrificed when clinical signs of illness were observed.

Recovery of Tumor Cells. Tumors were dispersed into single-cell suspensions by treatment of minced tissue with collagenase (2000 units/ml, Sigma) in RPMI 1640 medium for 30 min at 37°C. Undigested tissue was removed and dead cells and cell debris were eliminated by using Ficoll/Hypaque (Sigma) density centrifugation. Cell preparations were then sampled for RNA extraction or for flow cytofluorometry (FCF) analysis. Tissue samples from tumors were fixed in phosphate-buffered formalin and were paraffin-embedded. Sections (4 μm) were stained with hematoxylin and eosin and examined with a light microscope for histopathology.

Immunofluorescence (IF) Staining and FCF Analysis. The following monoclonal antibodies (mAbs) were used for cell surface phenotyping: anti-CD19 (B4, Coulter), anti-CD21 (HB5, American Type Culture Collection), anti-CD23 (BU38, The Binding Site, Birmingham, U.K.), anti-CD38 (OKT10, Ortho Diagnostics), anti-CD11a/18 (LFA-1; M10157-OAX, Pel-Freez Biologicals), anti-CD54 (ICAM-1; RR1/1; T. Springer, Dana–Farber, Boston), and anti-CD58 (LFA-3; TS2/9.1; T. Springer). Fluorescein isothiocyanate-conjugated polyclonal goat anti-mouse immunoglobulin was used as the second label. The presence of contaminating mouse cells was excluded by differential staining with W6/32 (American Type Culture Collection) for HLA class I antigen and with anti-H-2k^d (Pharmingen, San Diego) for mouse H-2 class I antigen. Two-color IF staining was done using a fluorescein isothiocyanate-conjugated anti-CD23 mAb (The Binding Site) and a phycoerythrin-conjugated anti-CD38 mAb (Ortho Diagnostics). LCLs and the corresponding tumor cells were analyzed for surface marker expression using a FACS IV analyzer or FACScan as described (24) and the data were analyzed with LYSIS II software (Becton Dickinson).

Cell Cycle Analysis. LCLs and tumor cells were stained with acridine orange (Polysciences) and were analyzed with the FACS IV exactly as described (24). The data were analyzed with LYSIS II software and were presented as bivariate contour plots of red (RNA) vs. green (DNA) fluorescence.

Recombinant Clones. DNA fragments specific for each gene were generated by PCR of LCL cDNA using the GeneAmp PCR kit (Perkin–Elmer/Cetus). The PCR products were first cloned into the pCR vector (Invitrogen, San Diego) and then subcloned into pGem-4 (Promega) (LMP1 and CD23) or were directly cloned into pGem-4 [ribosomal protein (rp) L32 and EBNA2]. Insert orientation was for antisense RNA synthesis from the flanking T7 promoter. Fragment orientation and sequence authenticity were verified by dideoxynucleotide sequencing (Sequenase; United States Biochemical). The following clones were prepared: EBNA2 [nucleotides (nt) 980–1275 (25)], LMP1 [nt 1111–1440 (26)], CD23 [nt 701–920 (27)], and rpL32 [nt 60–135 (28)].

RNase Protection Assay. RNA was extracted from tumor cells or LCLs by using the one-step method of Chomczynski and Sacchi (29). Antisense RNA, generated from *Eco*RI-linearized templates, was synthesized with T7 polymerase, the Riboprobe Gemini core system (Promega), and [^{32}P]UTP (3000 Ci/mmol; 1 Ci = 37 GBq; Amersham) as the labeled nucleotide. The RNA from 1.5×10^6 cells was hybridized with a multiple probe set containing antisense RNA probes specific for CD23, rpL32, EBNA2, and LMP1. Hybridization reactions, RNase treatment, and isolation of protected RNA·RNA duplexes were done as essentially described by Melton *et al.* (30) with the exception of using only RNase T1. Final samples were electrophoresed in 5% polyacrylamide/8 M urea gels and visualized by autoradiography. Densitometric analysis of autoradiograms was done using an Ultroscan XL densitometer (Pharmacia LKB).

ELISA. Sandwich ELISA was done to detect immunoglobulin in serum and in culture supernatants. Microwell plates were coated (100 μl per well) with the capture antibody (goat anti-human μ, γ, and α; Zymed Laboratories) diluted to 1 μg/ml. Serum from mice taken at the time of sacrifice or supernatant from a 48-h culture of 1×10^6 cells was added at various dilutions. The standard was a pool of human IgM, IgG, and IgA myeloma proteins (provided by H. Spiegelberg, University of California, San Diego, La Jolla, CA). The detecting antibody was alkaline phosphatase-conjugated goat anti-human μ, α, and γ (Zymed Laboratories). The reaction was terminated by addition of 0.3 M NaOH and absorbance at 410 nm was measured (Dynatech model MR600 microplate reader).

RESULTS

By transferring LCLs into SCID mice, we were able to assess phenotypic changes associated with tumor formation by a well-characterized population of rapidly dividing EBV-infected cells. Five LCLs derived by *in vitro* transformation of mononuclear cells from five donors (EW, TL, LG, JR, and KR) were analyzed to determine whether the results were consistent for different LCLs or specific for a given LCL. Each LCL was transferred into at least four mice. All mice developed tumors. In addition, one cell line, JR, gave rise to both ascites and solid tumor masses. However, no phenotypic differences were observed between ascites and solid tumors. The length of time to debilitating tumor development was characteristic for each LCL and ranged from 18 days after injection (JR) to 38 days after injection (LG).

Morphologic examination of the tumors revealed immunoblastic lymphomas with a predominance of plasmacytoid cells (small nucleus, clock-like dispersed chromatin, large cytoplasm, and a single prominent nucleolus) and variable degrees of necrosis, similar to previous observations (17). This contrasts with the lymphoblastoid morphology of LCLs (small cell volume, high nucleus/cytoplasm ratio, and multiple prominent nucleoli) (data not shown). A high level of serum immunoglobulin was found in all mice at the time of sacrifice (9–31 mg/ml). This contrasts with the low level of immunoglobulin detected in 24-h supernatants from cultured LCLs (9–17 μg per ml per 10^6 cells). To verify that high levels of serum immunoglobulin originated in part from the tumor masses, dissociated fresh tumor cells and an equivalent number of matching LCLs from two donors (EW and TL) were placed in culture and the supernatant immunoglobulin was measured at 48 h. The levels of supernatant immunoglobulin in tumor cell culture were ≈3-fold higher than the levels in LCL cultures (26.6 ± 5.4 μg per ml per 10^6 cells vs. 9.7 ± 0.6 μg per ml per 10^6 cells, respectively), thus suggesting that the tumor cells have an altered potential for production of immunoglobulin compared to LCLs.

LCLs and Tumors Differ in Phenotype. To extend our observation that tumors have reduced expression of CD23 relative to donor-matched LCLs (21), we analyzed the expression of the following cell surface markers: HLA class I, CD19, CD21, CD23, CD38, CD11a (LFA-1), CD54 (ICAM-1), and CD58 (LFA-3). CD19 and CD21 are present through pre-B-cell and mature B-cell ontogeny (31). CD23 is expressed on EBV-infected or mitogen-stimulated B cells, but not on mature plasma cells (31, 32). CD38 is found only on pre-B cells and plasma cells, but not on activated B cells (31, 33). The adhesion molecules CD11a and CD58 are expressed during most stages of B-cell differentiation with the exception that expression decreases in plasma cells (34). Expression of CD54 is B-cell-lineage-specific and is only found on mature B cells and plasma cells (35). A representative FCF analysis of LG.LCL and matched tumor cells is shown in Fig. 1. Table 1 is a summary of the mean fluorescence intensities for analyzed pairs of four LCLs and tumor cells.

Clear phenotypic differences between the LCLs and matched tumor cells were observed. The expression of CD23, CD11a, and CD58 decreased in the tumor cells relative to the LCLs. In contrast, CD38 expression increased in the tumor cells relative to the LCLs. Surprisingly, the levels of HLA class I and CD54 (ICAM-1) were also higher in the tumor cells relative to the LCLs. The cell surface expression of CD19 and CD21 when calculated by the mean fluorescence intensities do not show statistically significant changes. The phenotype of the tumor cells is consistent with a plasma-cell phenotype. Reduced tumor-cell expression of CD11a, CD23, and CD58 was not a consequence of collagenase digestion of tumors, as collagenase treatment of control LCLs had no effect on expression (data not shown).

The B-cell markers CD23 and CD38 can be used to distinguish activated B cells from mature plasma cells. We performed a two-color FCF analysis to evaluate the coexpression of CD23 and CD38 by the LCLs and the matching tumor cells. The resulting contour plots (Fig. 2) reveal distinct differences between the two cell types. Whereas the predominant population (>80%) of LCLs expressed high levels of CD23 ($CD23^{hi}$) and low levels of CD38 ($CD38^{lo}$), the major population (>80%) of tumor cells expressed the reciprocal phenotype (i.e., $CD23^{lo}/CD38^{hi}$). These experiments were repeated for four transformed lines and the matched tumors with similar results (data not shown), thereby demonstrating that the phenotypic shift is a predominant event in this model.

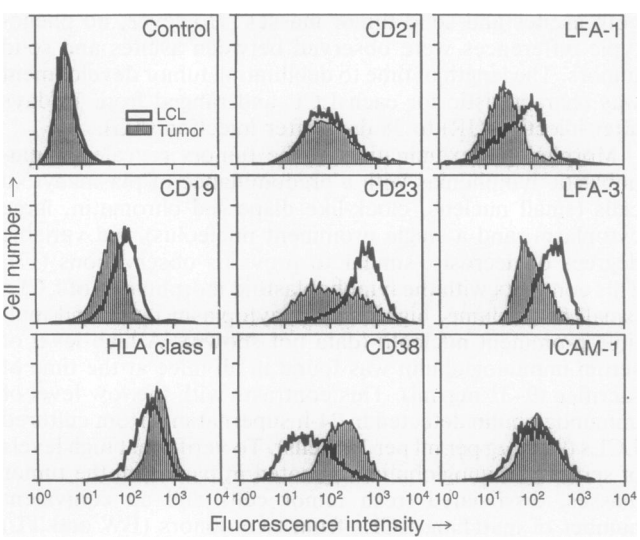

FIG. 1. Expression of B-cell surface markers. LCLs and tumor cells were examined by IF staining and FCF analysis for levels of HLA class I, CD19, CD21, CD23, CD38, CD11a (LFA-1), CD58 (LFA-3), and CD54 (ICAM-1). Overlapping fluorescence histograms are shown from LCLs (open peaks) and tumor cells (shaded peaks) stained for the markers indicated. Control indicates IF staining with secondary antibody alone.

Table 1. Mean fluorescence intensities of LCL and tumor cells

Marker	LCL, MFI	Tumor, MFI	*P*
Background	8 ± 2	11 ± 3	NS
HLA class I	378 ± 29	559 ± 15	<0.01
CD19	120 ± 18	108 ± 19	NS
CD21	324 ± 105	244 ± 26	NS
CD23	625 ± 48	204 ± 29	<0.01
CD38	58 ± 20	214 ± 43	<0.01
CD11a	201 ± 45	100 ± 33	<0.05
CD58	468 ± 91	254 ± 72	<0.01
CD54	185 ± 53	250 ± 49	<0.05

MFI, mean fluorescence intensity; NS, not significant. Data are expressed as the mean ± SEM. *P* values are from Student's *t* test for paired samples ($n = 4$).

Tumor Cells Are Predominantly in G_0/G_1 Phase. Terminal differentiation of cells is associated with gradual exit from the cell cycle (36). To assess the cell cycle status of freshly dispersed tumors cells and matched LCLs, we stained the cells with acridine orange and performed two-color FCF analysis. A contour plot, representative of four analyses (TL, JR, LG, and EW), is shown in Fig. 3. The LCLs yielded cell cycle profiles indicative of a rapidly dividing population, whereas the majority of tumor cells were restricted to G_0 and early G_1 phases. In addition, a striking decrease in the level of RNA is noted in the tumor cells relative to the LCLs. The contour plots of the tumor cells consistently reveal a small fraction of cells that falls outside of the cell cycle. This was observed for all tumors analyzed. We suspect that, due to the inherent "stickiness" of tumor cells, these populations probably represent aggregates. To confirm that the tumor cells have a decreased capacity to traverse S phase, TL.LCL and matched fresh tumor cells were cultured for 24 h, pulse-labeled for 4 h with [^{3}H]thymidine, and then analyzed for [^{3}H]thymidine uptake. [^{3}H]Thymidine uptake by the LCLs was ≈10-fold higher than thymidine uptake by the tumor cells (1.05×10^5 cpm per 10^5 cells vs. 1.36×10^4 cpm per 10^5 cells, respectively).

EBV Latent Gene Expression Is Reduced in Tumors. To determine whether the phenotypic changes observed in the tumor cells extended to changes in viral gene expression and to determine whether the decrease in CD23 surface expression corresponded to a decrease in mRNA levels, an RNase

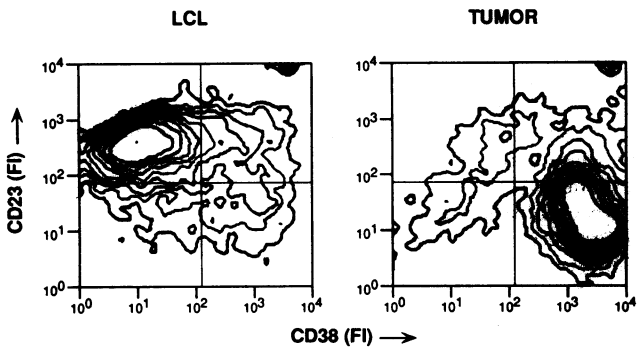

FIG. 2. Correlated expression of CD23 and CD38. Donor-matched LCLs and tumor cells were stained with fluorescein isothiocyanate-conjugated CD23 mAb and phycoerythrin-conjugated CD38 mAb and subjected to FCF analysis. Bivariated contour plots (10% probability scale) representing ≈5000 gated events are shown from a representative analysis (LG.LCL and LG.LCL tumor). FI, fluorescence intensity.

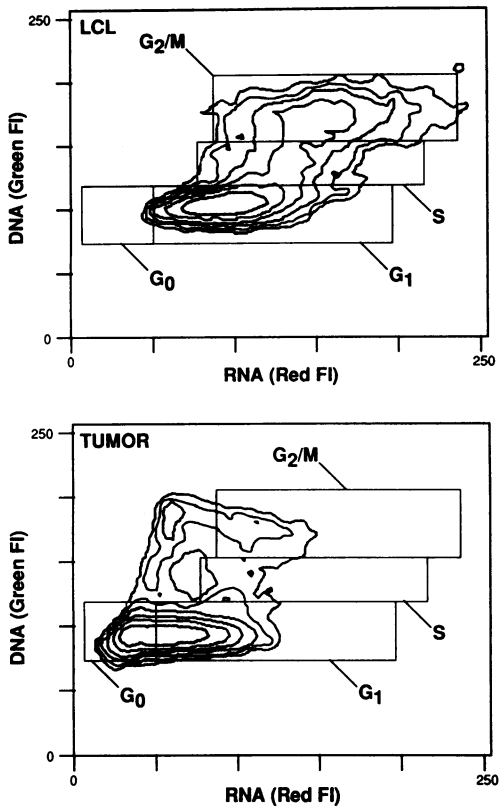

FIG. 3. Cell cycle analysis of LCLs and tumor cells. The marker settings used for cell cycle phases were as described (25). A 50% logarithmic contour plot representing ≈8500 gated events for the TL.LCL and the TL.LCL-derived tumor is shown. FI, fluorescence intensity.

protection assay was done to compare tumor cells and LCLs for levels of transcripts for CD23, EBNA2, LMP1, and a housekeeping gene, rpL32. RNA, extracted from equivalent numbers of cells, was used for hybridization to antisense probes to determine the amount of mRNA per cell. The results of a representative assay are shown in Fig. 4 and the quantitative analysis of the data from all experiments is shown in Fig. 5.

The levels of all measured transcripts were decreased in the tumor cells relative to the LCLs. The EBV latent genes LMP1 and EBNA2 have reduced expression in the tumor cells, with a mean 5-fold decrease measured (Fig. 5). The reduced expression was consistently observed in all mice as seen in Fig. 4, LCL tumors 1, 2, and 3. Consistent with the decrease in surface density of CD23 measured by flow cytometry, CD23 mRNA levels were 9-fold lower in tumor cells relative to the LCLs. Interestingly, rpL32 gene expression was also decreased in the tumor cells relative to the LCLs (3-fold), thus, suggesting that overall gene expression is reduced in tumor cells. If the densitometry analyses of EBNA2, LMP1, and CD23 are normalized to rpL32, the levels of EBNA2, LMP1, and CD23 RNAs were still significantly reduced in tumor cells relative to LCLs (2-fold for EBNA2 and LMP1 and 4-fold for CD23). In addition, when hybridization was based on total RNA rather than cell number, these differences were still observed (data not shown). The decrease in measured transcripts is not due to cell death, as only cell samples with >95% viability were used for RNA extraction.

DISCUSSION

EBV-associated B-cell LPDs constitute a frequent potentially lethal complication for individuals with disease-

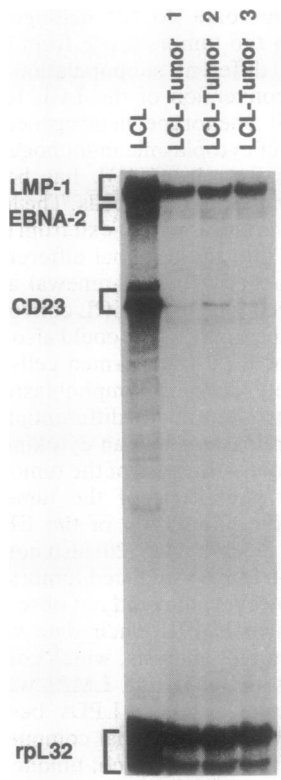

FIG. 4. Cellular and viral gene expression in LCLs and tumor cells. A multiprobe RNase protection assay was performed to detect cellular CD23, rpL32, and viral EBNA-2 and LMP-1 mRNA in LCLs and tumor cells. Tumor cells were taken from three mice. RNA from 1.5 × 10^6 cells was analyzed in each track.

associated or iatrogenic immunosuppression and compromised EBV-specific T-cell responses, most notably post-transplant patients. Human LPDs are thought to approximate *in vitro*-transformed LCLs (12, 37) but commonly exhibit features of plasmacytoid differentiation (13–16). In this study on the SCID/hu mouse model of human LPD, we demonstrate that EBV-infected tumor cells are predominantly plasmacytoid rather than LCL-like. This assertion is based on observed changes in cell morphology, the presence of plasma-cell-associated surface markers, increased levels of immunoglobulin secretion, and decreased proliferative activity. These changes were not unique to a given LCL since they were consistent for all lines analyzed. We also make the critical observation that plasmacytoid differentiation is associated with reduced expression of the EBV latent genes EBNA2 and LMP.

Our results suggest that EBV-immortalized cells terminally differentiate in an *in vivo* environment. This contrasts with the prevailing theory that EBV "fixes" B cells at the lymphoblastoid stage of EBV differentiation (38), which is characterized by the high level expression of the B-cell activation antigens and adhesion molecules (11) and by continuous

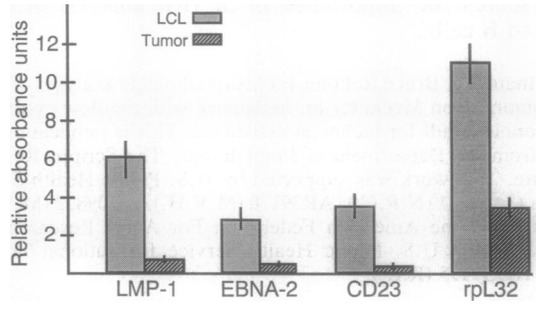

FIG. 5. Histogram of relative absorbance units from densitometric analysis of an RNase protection assay for the following RNAs: LMP-1, EBNA-2, CD23, and rpL32. The mean from LCLs (n = 4) or LCL-derived tumors (n = 10) is shown. The SEM is indicated by the bar.

proliferation in culture (39). Our data do not distinguish whether the plasma-like cells in the tumors arose from the outgrowth of a phenotypically different subpopulation of cells in the LCL or from the conversion of the LCL to a differentiated phenotype. B-cell phenotype heterogeneity, characterized by the expression of cytoplasmic immunoglobulin (40) and PC1 [a plasma cell antigen (41)], has been observed in LCLs, but only in a minority of the cells. The low proliferation rate of the tumor cells and apparent exit from the cell cycle suggest that entrance into the terminal differentiation pathway eliminates the capacity for self-renewal and argues that the lymphoblastoid cell type in the LCL converts to the plasma cell phenotype in the tumor. This could also be occurring *in vitro* but passage of EBV-transformed cells in culture would select for actively dividing lymphoblastoid cells. Alternatively, conversion to a terminally differentiated phenotype could be due to the release of human cytokines, such as interleukin 6, in the microenvironment of the tumors.

The terminally differentiated phenotype of the tumors correlates with a reduction in the expression of the EBV latent genes EBNA2 and LMP1. Picchio *et al.* (20) also noted a reduction in EBNA2 expression in EBV-induced tumors in SCID mice relative to LCLs. However, they did not observe a similar decrease in the levels of LMP1. Their data was based on a less-sensitive Western blot analysis, which could explain the difference in results. EBNA2 and LMP1 were also not detected in several samples of human LPDs, based on Western blot analysis (J. McKnight, personal communication), suggesting that these observations are not unique to the SCID mouse model.

We show that CD23 expression is decreased in the tumors at the level of cell surface expression and mRNA accumulation. EBNA2 expression has been shown to transcriptionally upregulate CD23 expression (42). This would suggest that the decrease in CD23 we observed is caused by the reduction in EBNA2 expression. Alternatively, reduced CD23 and EBNA2 may be independently related to B-cell differentiation, as the $CD23^{lo}/CD38^{hi}$ phenotype has been identified by FCF analysis of normal human plasma cells (43). Interestingly, expression of LMP1 has been correlated with an increased expression of CD11a, CD54, and CD58 after LMP gene transfer into EBV-negative Burkitt lymphoma cells (44). However, in association with reduced LMP1 in the tumors, we observed a decrease in expression of CD11a and CD58, but not CD54, suggesting that expression of adhesion molecules is also independently regulated and related to differentiation.

The tumors from EBV-induced LPD in SCID mice have been shown to be remarkably similar to human LPD (17, 19). In this study, we clearly show SCID tumors differ phenotypically from *in vitro*-transformed LCLs. Of particular note, the differentiation-associated reduction in EBV latent gene expression may play a role in the pathogenesis of LPD and underscores the importance of *in vivo* analysis of EBV-infected B cells.

We thank Dr. Bruce Robbins for histopathologic analyses of LCLs and tumors, Don McQuitty for assistance with the flow cytometry, and Bonnie Bradt for technical assistance. This is publication 7477 IMM from the Department of Immunology, The Scripps Research Institute. This work was supported by U.S. Public Health Service Grants CA52241 (N.R.C.), AR39178 (M.V.H.), AG09822 (M.V.H.), a grant from the American Federation For Aging Research, Inc. (M.V.H.), and U.S. Public Health Service Institutional Training Grant HLO7195 (R.R.).

1. Thomas, J. A., Allday, M. J. & Crawford, D. H. (1991) *Adv. Cancer Res.* **57**, 329–380.
2. Hanto, D. W., Frizzera, G., Gajl-Peczalska, K. & Simmons, R. L. (1985) *Transplantation* **39** (5), 461–472.
3. Ho, M., Miller, G., Atchison, R. W., Breinig, M. K., Dummer, J. S., Andiman, W., Starzl, T. E., Eastman, R., Griffith, B. P., Hardesty, R. L., Bahnson, H. T., Hakala, T. R. & Rosenthal, J. T. (1985) *J. Infect. Dis.* **152**, 876–886.
4. Kieff, E. & Liebowitz, D. (1990) in *Virology*, eds. Fields, B. N. & Knipe, D. M. (Raven, New York), pp. 1889–1920.
5. Sugden, B. & Warren, N. (1989) *J. Virol.* **63**, 2644–2649.
6. Yates, J. L., Warren, N. & Sugden, B. (1985) *Nature (London)* **313**, 812–815.
7. Dambaugh, T., Wang, F., Hennessy, K., Woodland, E., Rickinson, A. & Kieff, E. (1986) *J. Virol.* **59**, 453–462.
8. Hammerschmidt, W. & Sugden, B. (1989) *Nature (London)* **340**, 393–397.
9. Wang, D., Liebowitz, D. & Kieff, E. (1985) *Cell* **43**, 831–840.
10. Wang, F., Gregory, C., Sample, C., Rowe, M., Liebowitz, D., Murray, R., Rickinson, A. & Kieff, E. (1990) *J. Virol.* **64** (5), 2309–2318.
11. Calender, A., Billaud, M., Aubry, J.-P., Banchereau, J., Vuillaume, M. & Lenoir, G. M. (1987) *Proc. Natl. Acad. Sci. USA* **84**, 8060–8064.
12. Young, L., Alfieri, C., Hennessy, K., Evans, H., O'Hara, C., Anderson, K. C., Ritz, J., Shapiro, R. S., Rickinson, A., Kieff, E. & Cohen, J. I. (1989) *N. Engl. J. Med.* **321** (16), 1080–1085.
13. Thomas, J. A., Hotchin, N. A., Allday, M. J., Amlot, P., Rose, M., Yacoub, M. & Crawford, D. H. (1990) *Transplantation* **49** (5), 944–953.
14. Frizzera, G., Hanto, D. W., Gajl-Peczalska, K. J., Rosai, J., McKenna, R. W., Sibley, R. K., Holahan, K. P. & Lindquist, L. L. (1981) *Cancer Res.* **41**, 4262–4279.
15. Nalesnik, M. A., Jaffe, R., Starzl, T. E., Demetris, A. J., Porter, K., Burnham, J. A., Makowka, L., Ho, M. & Locker, J. (1988) *Am. J. Pathol.* **133** (1), 173–192.
16. Randhawa, P. S., Samuel, A., Yousem, S. A., Paradis, I. L., Dauber, J. A., Griffith, B. P. & Locker, J. (1989) *Am. J. Pathol.* **92** (2), 177–185.
17. Cannon, M. J., Pisa, P., Fox, R. I. & Cooper, N. R. (1990) *J. Clin. Invest.* **85**, 1333–1337.
18. Rowe, M., Young, L. S., Crocker, J., Stokes, H., Henderson, S. & Rickinson, A. B. (1991) *J. Exp. Med.* **173**, 147–158.
19. Pisa, P., Cannon, M. J., Pisa, E. K., Cooper, N. R. & Fox, R. I. (1992) *Blood* **79** (1), 173–179.
20. Picchio, G. R., Kobayashi, R., Kirven, M., Baird, S. M., Kipps, T. J. & Mosier, D. E. (1992) *Cancer Res.* **52**, 2468–2477.
21. Garnier, J. L., Cooper, N. R. & Cannon, M. J. (1992) *Am. J. Pathol.*, in press.
22. Rickinson, A. B., Rowe, M., Hart, I. J., Yao, Q. Y., Henderson, L. E., Rabin, H. & Epstein, M. A. (1984) *Cell. Immunol.* **87**, 646–658.
23. Bosma, G. C., Custer, R. P. & Bosma, M. J. (1983) *Nature (London)* **301**, 527–530.
24. Ernst, D. N., McQuitty, D. N., Weigle, W. O. & Hobbs, M. V. (1988) *Cell. Immunol.* **114**, 161–173.
25. Sample, J., Hummel, M., Braun, D., Birkenbach, M. & Kieff, E. (1986) *Proc. Natl. Acad. Sci. USA* **83**, 5096–5100.
26. Hatfull, G., Bankier, A. T., Barrell, B. G. & Farrell, P. J. (1988) *Virology* **164**, 334–340.
27. Kikutani, H., Inui, S., Sato, R., Barsumian, E. L., Owaki, H., Yamasaki, K., Kaisho, T., Uchibayashi, N., Hardy, R. R., Hirano, T., Tsunasawa, S., Sakiyama, F., Suemura, M. & Kishimoto, T. (1986) *Cell* **47**, 657–665.
28. Young, J. A. T. & Trowsdale, J. (1985) *Nucleic Acids Res.* **13** (24), 8883–8891.
29. Chomczynski, P. & Sacchi, N. (1987) *Anal. Biochem.* **162**, 156–159.
30. Melton, D. A., Krieg, P. A., Rebagliati, M. R., Maniatis, T., Zimm, K. & Green, M. R. (1984) *Nucleic Acids Res.* **12**, 7035–7056.
31. Uckun, F. (1990) *Blood* **76**, 1908–1923.
32. Thorley-Lawson, D. A., Nadler, L. M., Atul, K. B. & Schooley, R. T. (1985) *J. Immunol.* **134** (5), 3007–3012.
33. Anderson, K. C., Park, E. K., Bates, M. P., Leonard, R. C., Hardy, R., Schlossman, S. F. & Nadler, L. M. (1983) *J. Immunol.* **130**, 1132–1138.
34. Ahsmann, E. J. M., Lokhorst, H. M., Dekker, A. W. & Bloem, A. C. (1992) *Blood* **79** (8), 2068–2075.
35. Boyd, A. W., Dunn, S. M., Fecondo, J. V., Culvenor, J. G., Duhrsen, U., Burnes, G. F. & Wawryk, S. O. (1989) *Blood* **73** (7), 1896–1903.
36. Crocker, J. (1989) *Clin. Exp. Immunol.* **77**, 299–308.
37. Rickinson, A. B. (1991) in *Transplantation and Clinical Immunology*, eds. Touraine, J. L., Traeger, J., Betuel, H., Dubernard, J. M., Revillard, J. P. & Dupuy, C. (Elsevier, Amsterdam), pp. 247–253.
38. Thorley-Lawson, D. A. & Mann, K. P. (1985) *J. Exp. Med.* **162**, 45–59.
39. Pope, J. H., Horne, M. K. & Scott, W. (1968) *Int. J. Cancer* **3**, 857–866.
40. Wendel-Hansen, V., Rosen, A. & Klein, G. (1987) *Int. J. Cancer* **39**, 404–408.
41. Crawford, D. H. & Ando, I. (1986) *Immunology* **59**, 405–409.
42. Wang, F., Gregory, C. D., Rowe, M., Rickinson, A. B., Wang, D., Birkenbach, M., Kikutani, H., Kishimoto, T. & Kieff, E. (1987) *Proc. Natl. Acad. Sci. USA* **84**, 3452–3456.
43. Terstappen, L. W. M. M., Johnsen, S., Segers-Nolten, M. J. & Loken, M. R. (1990) *Blood* **76** (9), 1739–1747.
44. Wang, D., Liebowitz, D., Wang, F., Gregory, C., Rickinson, A., Larson, R., Springer, T. & Kieff, E. (1988) *J. Virol.* **62**, 4173–4184.